

## Plant-wide modelling and analysis of WWTP temperature dynamics for sustainable heat recovery from wastewater

Magnus Arnell <sup>a,b,\*</sup>, Marcus Ahlström<sup>b</sup>, Christoffer Wärff <sup>a,b</sup>, Ramesh Saagi <sup>a</sup> and Ulf Jeppsson <sup>a</sup>

<sup>a</sup> Division of Industrial Electrical Engineering and Automation (IEA), Department of Biomedical Engineering, Lund University, P.O. Box 118, SE-22100 Lund, Sweden

<sup>b</sup> Unit of Urban Water Management, RISE Research Institutes of Sweden, Gjuterigatan 1D, SE-58273 Linköping, Sweden

\*Corresponding author. E-mail: magnus.arnell@iea.lth.se

 MA, 0000-0003-1547-8413

### ABSTRACT

Wastewater heat recovery upstream of wastewater treatment plants (WWTPs) poses a risk to treatment performance, i.e. the biological processes. In order to perform a sustainability analysis, a detailed prediction of the temperature dynamics over the WWTP is needed. A comprehensive set of heat balance equations was included in a plant-wide process model and validated for the WWTP in Linköping, Sweden, to predict temperature variations over the whole year in a temperate climate. A detailed model for the excess heat generation of biological processes was developed. The annual average temperature change from influent to effluent was 0.78 °C with clear seasonal variations; 45% of the temperature change arises from processes other than the activated sludge unit. Hence, plant-wide energy modelling was necessary to predict in-tank temperature in the biological treatment steps. The energy processes with the largest energy gains were solar radiation and biological processes, while the largest losses were from conduction, convection and atmospheric radiation. Tanks with large surface areas have a significant impact on the heat balance regardless of biological processes. Simulating a 3 °C lower influent temperature, the temperature in the activated sludge unit dropped by 2.8 °C, which had a negative impact on nitrogen removal.

**Key words:** energy and heat balance, mathematical modelling, resource recovery, temperature, wastewater heat recovery, wastewater treatment plant

### HIGHLIGHTS

- The annual average temperature change ( $\Delta T$ ) was +0.78 °C from influent to effluent.
- Biological processes had the largest energy contribution.
- 45% of  $\Delta T$  arises from other processes than activated sludge. Hence, plant-wide energy modelling is necessary.
- $\Delta T$  shows strong seasonal variation in colder climates. Dynamic parameters are necessary.
- Tanks with large open surface areas have significant impact on the heat balance.

### INTRODUCTION

As resource recovery from wastewater (WW) is widely applied to improve sustainability of wastewater treatment (WWT) systems (Verstraete *et al.* 2009), wastewater heat recovery (WWHR) is gaining wider interest (Culha *et al.* 2015; Ceconet *et al.* 2020; Wärff *et al.* 2020). The energy in the WW largely comes from domestic hot water. According to several international studies, the energy use in the urban water cycle adds up to 10% or more of the total national energy use (Olsson 2012). Out of this only about 10% (corresponding to 1% of the total energy use) is used for withdrawal, treatment and distribution of tap water and collection, treatment and discharge of wastewater. The remaining part – the absolute majority – is used by the customers mainly for heating tap water for showers, dishwashers and laundry (Olsson 2012). The Swedish Energy Agency (2009) has estimated the heat requirement in households for domestic hot water (DHW) to be 1,150 kWh/cap/yr. This contributes to an elevated temperature of wastewater compared to tap water. Wastewater heat recovery (WWHR) is a known practice in many countries. It can be implemented either upstream of the wastewater treatment plant (WWTP), such as in showers, in building sewer stems, in sewer mains, or at the WWTP effluent after treatment

This is an Open Access article distributed under the terms of the Creative Commons Attribution Licence (CC BY 4.0), which permits copying, adaptation and redistribution, provided the original work is properly cited (<http://creativecommons.org/licenses/by/4.0/>).

(Arnell *et al.* 2017). From an energy recovery point of view, the more upstream locations are more favourable (i.e. they have a higher WW temperature). Conversely, more downstream locations have larger and more stable flows while the temperature at the same time is lower due to energy loss in the sewer network and mixing with intrusive water of lower temperature. This, along with maintenance concerns, makes passive heat exchangers more common in appliances and buildings while heat pumps are used in precincts or at WWTP effluents (Culha *et al.* 2015; Ceconet *et al.* 2020; Jonsson *et al.* 2020). Recovering heat from WW upstream of the WWTP will impact the influent temperature of the WW. Preliminary studies indicate that this effect is in the range 1–3 °C (Arnell *et al.* 2017).

Temperature is well known to impact performance and efficiency of WWT processes. Most processes are somewhat temperature dependent with density, viscosity and other basic characteristics of fluids varying with temperature. However, biological processes are the most sensitive within the temperature range WWTPs that operate at in temperate climates, 6–27 °C (la Cour Jansen *et al.* 1992; Henze *et al.* 2002). Rates of biological processes are reduced as temperature drops. At WWTPs with biological nitrogen removal, nitrification is the rate limiting process (Henze *et al.* 2008). From 20 to 10 °C, the maximum (i.e. non-limited by for example dissolved oxygen concentration) nitrification rate is reduced by more than 50% (Henze *et al.* 2002; Gernaey *et al.* 2014). Consequently, there is a risk that upstream recovery of heat from wastewater deteriorates the nitrogen removal at the WWTP and leads to higher discharges of nitrogen compounds to the environment or a higher consumption of energy and other resources at the plant to maintain the same effluent quality. The risk will depend on local conditions, such as size and quality of the sewer network and WW load relative to the design capacity of the plant. Therefore, the risk must be evaluated case by case before allowing WWHR in the catchment. To assess the plant performance as a function of temperature, process modelling and simulation can be used. Plant-wide modelling has been shown to be instructive for analysing energy use and recovery at WWTPs (Fernandez-Arevalo *et al.* 2017; Zaborowska *et al.* 2021). The bioprocess models used in research and industry, e.g. the Activated Sludge Models (ASM1, 2, 3) (Henze *et al.* 2000) or in commercial simulation platforms, include temperature dependency for the biological reactions.

However, the temperature across the WWTP is not constant. Solar radiation, wind, ambient temperature etc. can heat or cool uncovered tanks at WWTPs and studies have shown a temperature change of 1–2 °C from influent to effluent (la Cour Jansen *et al.* 1992; Makinia *et al.* 2005; Fernandez-Arevalo *et al.* 2014). In the published literature, several examples of how to model temperature, i.e. perform an energy balance, in WWTP tanks have been presented. In a pioneering work, la Cour Jansen *et al.* (1992) assessed the problem of operating nitrifying WWTPs in a cold climate. A temperature model for an activated sludge tank was presented based on a simple energy balance including the significant energy influences. The model was integrated with an ASM1 process model and validated against a one-year data set from one Danish WWTP. Sedory & Stenstrom (1995) presented a temperature model for an aeration basin and validated it for five North American WWTPs. Thirty-day temperature series for different temperature intervals were used as inputs to the model. Temperatures ranged from 12 to 31 °C and their model did not consider the effects on WWT performance. Their model accuracy was in the range 2–3 °C and did not predict extreme variations very well. In a more recent paper, Makinia *et al.* (2005) developed a temperature model for an activated sludge tank and compared a partial differential equation formulation with the more common ‘tanks in series’ approach. The model was tested for a short (a few days) data series with a temperature around 19 °C and did not consider WWTP performance. Lippi *et al.* (2009) sought to improve the temperature model from Sedory & Stenstrom (1995). The heat flux equations were updated to more detailed alternatives. When the model was tested against the same five data sets and a few more, the model accuracy was improved. However, the model still only covered an aeration basin and did not consider the impact on other treatment processes.

Considering two facts: (1) heat recovery is of most interest in areas with a cold climate and (2) the impact of WWHR on influent temperature is in the same range as the temperature change over the WWTP, a plant-wide process model including heat balances for temperature prediction is needed. The model must integrate process performance and temperature prediction and be proven valid for relevant climate and temperature conditions. Simulations for extended (full year) time periods are required to assess the impact and potential of WWHR in WW systems. Such a model has previously not been presented in the literature.

For this study, a novel plant-wide dynamic temperature model has been developed and implemented in a general process model framework. Modelled processes include grit chambers, pre-aeration tanks, primary clarifiers, activated sludge tanks, secondary settlers, tertiary biological and polishing (final clarifiers) steps and digesters. The temperature model has been developed and validated for a full year for a location with large temperature and climate variations in a temperate climate zone (Linköping, Sweden). The model was used to assess the impact of temperature change due to upstream wastewater heat recovery in various scenarios.

## METHODS

### General plant-wide temperature model

To model temperature over the plant and in each sub-process, Equation (1) was used. The net heat flux ( $\phi_n$ ) must be modelled including all relevant energy gains and losses. The heat flux equation (Equation (2)) was used as a basis for the model (Makinia *et al.* 2005),

$$\frac{dT_i}{dt} = \left(\frac{Q_i}{V_i}\right)T_{i-1} - \left(\frac{Q_i}{V_i}\right)T_i + \frac{\phi_n}{\rho_l C_{p,w} V_i} \quad (1)$$

where,  $T$  is the water temperature [°C];  $Q_i$  is the flow [ $\text{m}^3/\text{d}$ ];  $V_i$  is the reactor volume [ $\text{m}^3$ ];  $\phi_n$  is the net heat flux [ $\text{J}/\text{d}$ ];  $\rho_l$  is the liquid density [ $\text{kg}/\text{m}^3$ ]; and  $C_{p,w}$  is the specific heat capacity of water at constant pressure [ $\text{J}/(\text{kg K})$ ]. Index  $i$  represents the reactor number for a number of tanks in series:

$$\phi_n = \phi_{sr} - \phi_{ar} + \phi_c - \phi_e - \phi_a + \phi_m + \phi_{bp} \quad (2)$$

The components of the heat flux are the following:  $\phi_{sr}$  is solar radiation;  $\phi_{ar}$  is atmospheric radiation;  $\phi_c$  is conduction and convection;  $\phi_e$  is evaporation;  $\phi_a = \phi_{as} + \phi_{al}$  is aeration, sensible and latent heat losses;  $\phi_m$  is mechanical energy (not included); and  $\phi_{bp}$  represents biological processes.

Mathematical relations describing the included heat flux components were developed and selected based on the model objective, i.e. plant-wide temperature modelling for full year simulations of a WWTP in a temperate climate. The large span in water and air temperatures forced the use of dynamic expressions for most parameters. The full list of parameters is presented in Table 1 and in the Supplementary Information (S.I.). The separate model expressions for the heat flux components are presented in Equations (3)–(10).

The short-wave net radiation (solar radiation,  $\phi_{sr}$  [ $\text{J}/\text{d}$ ]) can be calculated from direct measurements of solar radiation using a local weather station or collected from a meteorological measuring station sufficiently close to the plant as:

$$\phi_{sr} = 86,400 \cdot SR \cdot A_s \quad (3)$$

where,  $SR$  is the solar radiation [ $\text{W}/\text{m}^2$ ];  $A_s$  is the tank area exposed to the atmosphere [ $\text{m}^2$ ]; and 86,400 is a time conversion factor [ $\text{s}/\text{d}$ ].

The long wave net radiation (atmospheric radiation,  $\phi_{ar}$  [ $\text{J}/\text{d}$ ]) is based on the Stefan–Boltzmann law and is given by the following expression,

$$\phi_{ar} = 86,400 \cdot [\varepsilon_{ar} \cdot \sigma \cdot T_w^{*4} - (1 - \lambda_{ar}) \cdot \sigma \cdot T_a^{*4} \cdot \beta_{ar}] \cdot A_s \quad (4)$$

where,  $\varepsilon_{ar}$  is the emissivity of the water surface [-];  $\sigma$  is the Stefan–Boltzmann constant [ $\text{W}/(\text{m}^2 \text{K}^4)$ ];  $\lambda_{ar}$  is the water surface reflectivity [-];  $T_a^*$  is the absolute temperature of the ambient air [K];  $T_w^*$  is the absolute temperature of the water surface [K]; and  $\beta_{ar}$  is the atmospheric radiation factor [-].

Surface convection ( $\phi_c$  [ $\text{J}/\text{d}$ ]) can be modelled as a function of wind speed and the temperature difference between the mass of water and the air above it according to Lippi *et al.* (2009):

$$\phi_c = 86,400 \cdot h \cdot (T_a^* - T_w^*) \cdot A_s \quad (5)$$

where,  $h$  is the heat transfer coefficient [ $\text{W}/(\text{m}^2 \text{K})$ ] and  $T_w^*$  is the absolute temperature of the water surface [K]. For the presented model, a temperature-dependent parameter expression has been adopted and implemented for Equation (5) in addition to the description by Lippi *et al.* (2009), see Table 1.

For the heat flux for evaporation ( $\phi_e$  [ $\text{J}/\text{d}$ ]) Equation (6) was used (Lippi *et al.* 2009):

$$\phi_e = 86,400 \cdot h_m \cdot A_s \cdot h_{fg}(\rho_{v,Ta} - \rho_{v,Tw}) \quad (6)$$

**Table 1** | List of values and expressions for included parameters

Parameter <sup>a</sup>	Heat flux component	Value/Equation <sup>a</sup>	Comment/Reference
$\varepsilon_{ar}$ [-]	$\phi_{ar}$	0.97	Makinia <i>et al.</i> (2005)
$\sigma$ [W/(m <sup>2</sup> K <sup>4</sup> )]	$\phi_{ar}$	$5.67 \cdot 10^{-8}$	
$\lambda_{ar}$ [-]	$\phi_{ar}$	0.03	Makinia <i>et al.</i> (2005)
$\beta_{ar}$ [-]	$\phi_{ar}$	0.95	Makinia <i>et al.</i> (2005)
$h$ [W/(m <sup>2</sup> K)]	$\phi_c$	$\frac{Nu \cdot k}{L_c}$	$L_c$ is dependent on tank size and geometry.
$Nu$ [-]	$\phi_c$	$(0.037 \cdot Re^{4/5} - 871) \cdot Pr^{1/3}$	
$k$ [W/(m K)]	$\phi_c$	$(251.626 + 7.734 \cdot T_a^* + 167.6 \cdot x_{zw} - 7.432 \cdot 10^{-4} \cdot T_a^* \cdot x_{zw} + 8.631 \cdot 10^{-6} \cdot T_a^{*2}) \cdot 10^{-5}$	Tsilingiris (2018)
$Pr$ [-]	$\phi_c$	$\frac{C_{p,mix} \cdot \mu_{air}}{k}$	
$C_{p,vap}$ [J/(kg K)]	$\phi_c$	1905.7	At 20 °C. XSteam <sup>b</sup> .
$C_{p,mix}$ [J/(kg K)]		$C_{p,a} + \frac{0.622 \cdot p_{sat,vap,a}}{P - p_{sat,vap,a}} \cdot C_{p,vap}$	Tsilingiris (2018)
$Re$ [-]	$\phi_c, \phi_e$	$\frac{u_w \cdot L_c}{\mu_{air}^{v_i}}$	$v_i$ index $i$ equals <i>air</i> for $\phi_c$ and <i>vap</i> for $\phi_e$ .
$\nu_{air}$ [m <sup>2</sup> /s]	$\phi_c$	$\frac{\mu_{air}^{v_i}}{\rho_{air}}$	Dynamic expressions for $\mu_{air}$ adopted from Rasmussen (1997) and for $\rho_{air}$ from Bower & Saylor (2009). See S.I. for full expressions and parameters.
$h_m$ [m/s]	$\phi_e$	$\frac{Sh \cdot D_{AB}}{L_c}$	
$Sh$ [-]	$\phi_e$	$(0.037 \cdot Re^{4/5} - 871) \cdot Sc^{1/3}$	
$Sc$ [-]	$\phi_e$	$\frac{\nu_{vap}}{D_{AB}}$	
$\nu_{vap}$ [m <sup>2</sup> /s]	$\phi_e$	$\frac{\mu_{vap}}{\rho_{vap}}$	Dynamic expressions for $\mu_{vap}$ adopted from Huber <i>et al.</i> (2009). See S.I. for full expressions and parameters for $\mu_{vap}$ and $\rho_{vap}$ .
$D_{AB}$ [m <sup>2</sup> /s]	$\phi_e$	$-2.775 \cdot 10^{-6} + 4.479 \cdot 10^{-8} \cdot T_a^* + 1.656 \cdot 10^{-10} \cdot T_a^{*2}$	Regression model adopted from Nellis & Klein (2012), which is fitted to data by Bolz & Tuve (1976).
$h_{fg}$ [J/kg]	$\phi_e, \phi_{al}$	$2.453 \cdot 10^3$	Incropera <i>et al.</i> (2007)
$\rho_{v,Ta}$ [kg/m <sup>3</sup> ]	$\phi_e$	$\frac{p_{sat,vap,a} \cdot M_{vap}}{R \cdot T_a^*}$	
$\rho_{v,Tw}$ [kg/m <sup>3</sup> ]	$\phi_e$	$\frac{p_{sat,vap,w} \cdot M_{vap}}{R \cdot T_w^*}$	
$C_{p,a}$ [J/(kg K)]	$\phi_{as}$	1,014	At 20 °C.
$M_w$ [g/mol]	$\phi_{al}$	18.016	
$R$ [J/(mol K)]	$\phi_e, \phi_{al}$	8.3147	
$p_{vap,w}$ [Pa]	$\phi_{al}$	$RH \cdot p_{sat,vap,w}$	See S.I. for expression of $p_{sat,vap,w}$ .
$h_f$ [-]	$\phi_{al}$	1	
$p_{vap,a}$ [Pa]	$\phi_{al}$	$RH \cdot p_{sat,vap,a}$	See S.I. for expression of $p_{sat,vap,a}$ .
$\Delta H_{aer}$ [kJ/g COD]	$\phi_b$	-13.9	Blackburn & Cheng (2005)
$\Delta H_{nit}$ [kJ/g N]	$\phi_b$	-23.2	See S.I. for calculation.
$\Delta H_{denit}$ [kJ/g N]	$\phi_b$	-45.0	See S.I. for calculation.
$\beta_{aer}$ [-]	$\phi_b$	0.6	Henze <i>et al.</i> (2002)
$\beta_{aer}$ [-]	$\phi_b$	0.2	Henze <i>et al.</i> (2002)
$\beta_{aer}$ [-]	$\phi_b$	0.4	Henze <i>et al.</i> (2002)

See table note or nomenclature list for symbols not explained above. For further explanation and reference of selected parameter expressions see Supplementary Information.

<sup>a</sup> $T_a^*$  Absolute temperature of the ambient air above the water surface [K];  $Nu$  Nusselts number [-];  $Re$  Reynolds number [-];  $Pr$  Prandtl number [-];  $k$  thermal conductivity of water [W/(m K)];  $L_c$  characteristic length for reactor surface [m];  $C_{p,mix}$  specific heat capacity of moist air at ambient air temperature and humidity [J/(kg K)];  $u_w$  wind speed [m/s];  $\nu_{air}$  kinematic viscosity of humid air [m<sup>2</sup>/s];  $\mu_{air}$  dynamic viscosity of humid air [N s/m<sup>2</sup>];  $\rho_{air}$  density of humid air [kg/m<sup>3</sup>];  $Sh$  Sherwoods number [-];  $Sc$  Schmidts number [-];  $\nu_{vap}$  kinematic viscosity of water vapour [m<sup>2</sup>/s];  $D_{AB}$  binary mass diffusion coefficient [m<sup>2</sup>/s];  $p_{sat,vap,a}$  saturated vapour pressure at ambient air temperature [Pa];  $\mu_{vap}$  dynamic viscosity of water vapour [N s/m<sup>2</sup>];  $\rho_{vap}$  density of water vapour [kg/m<sup>3</sup>];  $M_{vap}$  mole weight for water vapour (=mole weight for water) [g/mol];  $T_w^*$  absolute temperature of the water [K];  $p_{sat,vap,w}$  saturated vapour pressure at water temperature [Pa]. COD, chemical oxygen demand.

<sup>b</sup>Data obtained with X Steam Software. An implementation of the IAPWS IF97 standard for MATLAB.

where,  $h_m$  is the mass transfer coefficient [m/s];  $h_{fg}$  is the latent heat of vapourization of water [J/kg];  $\rho_{v,T_a}$  is the saturated vapour density at the ambient air temperature [kg/m<sup>3</sup>]; and  $\rho_{v,T_w}$  is the saturated vapour density at the water surface temperature [kg/m<sup>3</sup>]. The applicability of Equation (6) was improved by adopting dynamic expressions for essential parameters, see Table 1.

Heat loss from aeration ( $\phi_a$  [J/d]) is modelled as the sum of sensible heat loss ( $\phi_{as}$  [J/d]) and latent heat loss ( $\phi_{al}$  [J/d]), which is given by the following expressions (Makinia *et al.* 2005):

$$\phi_a = \phi_{as} + \phi_{al} \quad (7)$$

$$\phi_{as} = \rho_a \cdot C_{p,a} \cdot Q_a \cdot (T^* - T_a^*) \quad (8)$$

$$\phi_{al} = \frac{M_w \cdot Q_a \cdot h_{fg}}{R} \left\{ \frac{p_{vap,w} \cdot [RH + h_f \cdot (1 - RH)]}{T_w^*} - \frac{p_{vap,a} \cdot RH}{T_a^*} \right\} \quad (9)$$

where,  $\rho_a$  is the density of humid air [kg/m<sup>3</sup>];  $C_{p,a}$  is the specific heat capacity for air [J/(kg K)];  $Q_a$  is the air flow [m<sup>3</sup>/d];  $M_w$  is the mole weight of water [g/mol];  $R$  is the universal gas constant [J/(mol K)];  $RH$  is the relative humidity (decimal value) [-];  $p_{vap,w}$  is the vapour pressure at water temperature [Pa];  $h_f$  is the exit air humidity factor [-]; and  $p_{vap,a}$  is the vapour pressure of water at ambient air temperature [Pa].

A method to calculate the heat produced by exothermic biological reactions ( $\phi_{bp}$  [J/d]) was developed. The biological heat production from the degradation of organic matter (oxidation of carbon), nitrification and denitrification is calculated from the enthalpy of reaction ( $\Delta H$ ) of the chemical reactions (Henze *et al.* 2008; Kleerebezem & van Loosdrecht 2010). Dynamically calculated conversion rates in the process model were used:

$$\phi_{bp} = -((1 - \beta_{aer}) \cdot \Delta H_{aer} \cdot \Delta COD_{aer} + (1 - \beta_{nit}) \cdot \Delta H_{nit} \cdot \Delta N_{nit} + (1 - \beta_{denit}) \cdot \Delta H_{denit} \cdot \Delta N_{denit}) \quad (10)$$

where,  $\Delta COD_{aer}$  is the amount of COD that is used for aerobic respiration per day [g COD/d];  $\Delta N_{nit}$  is the amount of nitrogen that is nitrified per day [gN/d];  $\Delta N_{denit}$  is the amount of nitrogen that is denitrified per day [gN/d];  $\Delta H_{aer}$  is the enthalpy of reaction for aerobic respiration [J/gCOD];  $\Delta H_{nit}$  is the enthalpy of reaction for nitrification [J/gN];  $\Delta H_{denit}$  is the enthalpy of reaction for denitrification [J/gN];  $\beta_{aer}$  is the metabolic efficiency for COD respiration [-];  $\beta_{nit}$  is the metabolic efficiency for nitrification [-];  $\beta_{denit}$  is the metabolic efficiency for denitrification [-].

The enthalpy of reaction for aerobic respiration is not trivial to calculate theoretically and was adopted from Blackburn & Cheng (2005). The enthalpies of reaction for nitrification and denitrification can be calculated by combining the half reactions for each conversion step using tabulated numbers for their respective enthalpy of formation (Kleerebezem & van Loosdrecht 2010; Fernandez-Arevalo *et al.* 2014), see Supplementary Information for reactions and calculation of enthalpies. The included enthalpies describe the total free energy from the reactions of the substrates, i.e. both the enthalpy bound in biomass and enthalpy lost as heat (Henze *et al.* 2002, 2008; Griffiths 2012). The metabolic efficiency factors ( $\beta$ ) for each of the processes were used to compensate (Henze *et al.* 2002).

### Plant-wide model integration

For general purpose use, the developed temperature model was implemented in the Benchmark Simulation Model No. 2 (BSM2). The BSM2 is a modelling framework for benchmarking of process control using a standardised model set-up, plant layout, load profiles and simulation and evaluation procedure (Gernaey *et al.* 2014). The evaluation criteria include major cost items (e.g. aeration energy and carbon source addition) in an operational cost index.

The model code for the temperature model in BSM2 is made available through Github. See S.I. for further information.

### Case study Linköping wastewater treatment plant

The Linköping WWTP treats municipal and industrial wastewater (approximately 20% of annual organic load is industrial) from a total of 180,000 PE. The treatment train has primary treatment with grit removal, pre-aeration and chemically enhanced primary clarifiers; secondary biological treatment in three parallel activated sludge units (ASUs) with intermittent aeration; and finally, an advanced tertiary treatment with ozone for micro-pollutant degradation, post nitrification and denitrification in a moving bed biofilm reactor (MBBR) and post-precipitation and clarification. Mixed sludge is stabilized through a belt thickener and anaerobic digestion in three, interconnected digesters (i.e. with circular mixing inbetween). The sludge is

dewatered in screw presses and the supernatant is treated in a side stream SHARON process for nitrogen removal (Figure 1). All main tanks are uncovered.

A plant-wide process model for the WWTP was used for implementation and validation of the temperature model. The model framework from BSM2 was used as a basis for the model development (Gernaey *et al.* 2014). For the model set-up, the primary settler was modelled using an empirical mass balance model by Otterpohl & Freund (1992). A modified version of ASM1 was chosen for the activated sludge process (Gernaey *et al.* 2014) followed by a point-settler (with an added sludge blanket reactor volume to include settler denitrification) model for the secondary clarifier. For the ozonation, only COD degradation and oxygen addition was modelled, no micro-pollutant removal. The post nitrification process was modelled with a simplistic MBBR model assuming a fixed surface-based nitrification rate on the carriers limited by substrate and dissolved oxygen (DO) availability and adjusted for temperature. Post denitrification was modelled using the concept of apparent kinetics (Baeten *et al.* 2019), using a modified ASM1 where heterotrophic microorganisms grow on – and consequently are limited by – primarily  $\text{NH}_4\text{-N}$  and secondly  $\text{NO}_3\text{-N}$  using a switching function (Hiatt & Grady 2008). The clarifiers in the tertiary treatment were only included for temperature modelling. In the sludge line, the digestion process is modelled using ADM1 and the thickener and dewatering units are described by simple ideal separation models (Gernaey *et al.* 2014). The AD is heated with district heating to a constant 37 °C. The side stream nitrogen removal was simplistically modelled using fixed effluent levels and removal factors for the different components based on empirical relations with data. The model was rigorously calibrated and validated following established principles for characterization (Melcer *et al.* 2003) and the Good Modelling Practice scheme (Rieger *et al.* 2012) using two separate data sets. The model was implemented, and simulations were run in MATLAB/Simulink (MATLAB 2017b, The Mathworks Inc., Natwick, MA, USA, 2017).

At the plant, extensive data collection was first carried out for input characterization, calibration and validation of both the regular process model and the temperature model. Along with information about the plant (tank dimensions, machine equipment, control strategies, etc.) analytical and operational data were collected for calibration (1 April–1 May 2019) and validation (19 Sept. 2018–19 Sept. 2019). Secondly, for the temperature model, meteorological data (air temperature, relative humidity, wind speed, air pressure, rain and solar radiation) were recorded for the period 30 April 2019–28 April 2020 using a Davis Instruments Vantage Pro2™ (#6162-EU) wireless weather station installed at the wastewater treatment plant in Linköping. Temperature was measured for the whole or part of the period at the influent, ASU tanks, secondary effluent (part of time), ozonation effluent (part of time) and plant effluent. The measurement uncertainty for all water temperature measurements except for the influent was  $\pm 0.2$  °C. The influent temperature measurement uncertainty is not assessed but according to manufacturer specifications it should not exceed  $\pm 0.6$  °C. The plant effluent temperature data had a period of faulty measurements when the sensor was periodically out of the water (23 Aug.–26 Aug. 2019). These data were excluded from the evaluation. Meteorological data were lost for three shorter periods (9 d in June/July 2019, 2 d in Feb. and 1 h in March 2020) due to limited storage capacity in the logger. For those periods data from the most near-by sites of the Swedish Meteorological and Hydrological Institute (SMHI) were used to fill the gaps: station Malmslätt, Linköping for all

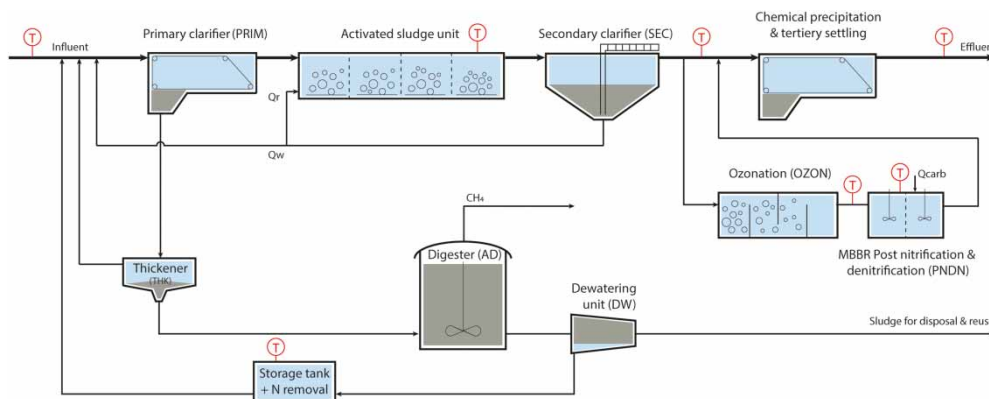


**Figure 1** | Model process flow diagram for the Linköping wastewater treatment plant. Temperature measurement positions are indicated in red. Side stream treatment SHARON process marked as 'Storage tank + N removal'. Please refer to the online version of this paper to see this figure in colour: <http://dx.doi.org/10.2166/wst.2021.277>.

meteorological parameters except solar radiation (approximately 10 km from WWTP) and station SMHI headquarters, Norrköping for solar radiation (approximately 40 km from WWTP).

The process model was calibrated following the procedures and stop criteria in the Good Modelling Practice protocol (Rieger *et al.* 2012). No calibration was performed for the temperature model in the sense of adjusting model parameters to improve the fit of the model. The resulting temperature profile for effluent water temperature of a full-year simulation was compared to data for validation of the model. Goodness of fit of the simulated effluent temperature to data for the validation period was calculated using Mean Absolute Error (*MAE*), Root Mean Squared Error (*RMSE*) and Square of Residuals ( $R^2$ ), as presented in Equations (11)–(13):

$$MAE = \sum \frac{|y - d|}{N} \quad (11)$$

$$RMSE = \sqrt{\sum \frac{(y - d)^2}{N}} \quad (12)$$

$$R^2 = 1 - \frac{\sum (d - y)^2}{\sum (d - \bar{d})^2} \quad (13)$$

where,  $y$  is the simulated data;  $d$  is the measured data;  $N$  is the number of observations; and  $\bar{d}$  is the average of the measured data.

Considering the intended use of the model – to evaluate the impact of influent temperature changes in the range 1–3 °C – the target for model accuracy (*MAE*) was set to 0.5 °C in the plant effluent.

### Simulation scenarios

The impact of WWHR upstream the WWTP was simulated by imposing a reduced influent temperature with 1, 2 and 3 °C in a series of three simulations (Scenarios 1, 2 and 3) to be compared with the validated reference case (Default case). Primarily, the nitrogen removal was evaluated in the activated sludge system and nitrogen concentrations at the plant effluent were compared to the effluent standards permitted.

## RESULTS AND DISCUSSION

### Plant-wide analysis of heat balance

The most relevant ambient meteorological data are shown in Figure 2. The summer period was relatively normal but the winter 2019/2020 was unusually warm with only very limited periods of really cold weather, i.e. with air temperatures below 0 °C (Figure 2(a)). As the location is relatively far to the north, the solar radiation is low or negligible during winter (Figure 2(b)). For this study, the meteorological data were collected on-site, providing the most accurate data for simulations. For example, solar radiation has a high local variability depending on cloud cover. Previous studies mostly used data from off-site meteorological stations, often many kilometres away from the plant (Sedory & Stenstrom 1995; Makinia *et al.* 2005; Lippi *et al.* 2009).

The overall prediction of the temperature change over the WWTP for the full-year simulation is plotted in Figure 3(a). Comparing the simulated effluent temperature with the measured values showed a good fit. The *MAE* was 0.30 °C, which is below the target of  $\pm 0.5$  °C. The *RMSE* equals 0.41 °C and the overall coefficient of determination  $R^2$  0.98. Minor deviations can be observed in Figure 3. There was a slight over prediction during the summer (Figure 3(b)), while the fit is generally better for the winter period (Figure 3(c)). At the end of the simulated period, as the temperature rises, model over prediction can be seen again. During model set-up, some fixed parameters used in previous studies (Makinia *et al.* 2005; Lippi *et al.* 2009) were exchanged for dynamic expressions (e.g.  $\rho_{air}$ ,  $\mu_{air}$  and  $D_{AB}$ ) to provide sufficient fit over the whole temperature range. This proves the necessity to validate the model for the full range of climate conditions for which it will be used to assure predictive power. A comparison of the modelled temperature in the ASU tanks with measured values in the same position is shown in Figure 4. The fit is good also in the ASU, however, the data show faulty behaviour in Figure 4(b) with frozen values followed by negative spikes at certain periods. The measurement uncertainty of  $\pm 0.2$  °C for the temperature sensors downstream of the influent was smaller than the model error and thus sufficiently accurate for the model validation. The relatively larger uncertainty of the influent temperature, up to  $\pm 0.6$  °C, propagate to the model results as it was used as input variable and thereby

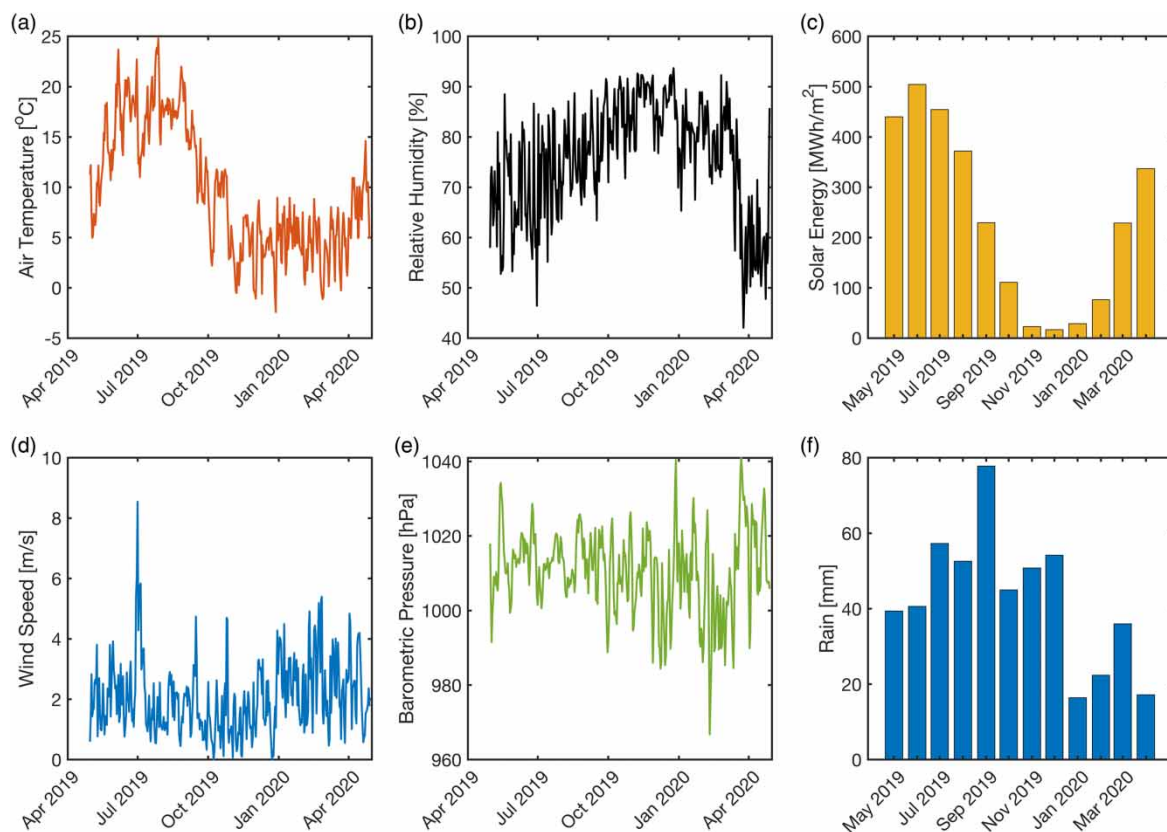


**Figure 2** | Overview of the most important variables in the meteorological data used in the model. (a) Air temperature (daily average), (b) relative humidity (daily average), (c) solar radiation (monthly total), (d) wind speed (daily average); (e) barometric pressure (daily average); and (f) rain (monthly total).

added to the overall model uncertainty. A general uncertainty analysis of all major input variables was not conducted in this study (Belia *et al.* 2009).

The net average temperature increase over the plant (from influent to effluent) for the full year was 0.78 °C (Figure 5(a)). However, seasonal variations occur (Figure 3). During the warmer period of the year, the change was larger – due to solar radiation – with a net increase in temperature (Figure 5(b)). For example, the temperature increased by 1.8, 1.4 and 1.2 °C for June, July, August 2019, respectively. During winter, the net changes were small, –0.13, –0.04 and –0.05 °C for November, December 2019 and January 2020, respectively. With minimal solar radiation in winter (Figure 2(c)), the energy contribution from the biological processes at this time of the year was not even compensating for the energy loss due to convection, evaporation, aeration etc. (Figure 6(b)). Studying the sub processes of the plant individually, the ASU was the one with the greatest impact on temperature (Figure 5(a)). Excluding the ASU, the average temperature change was 0.35 °C, or 45% of the total change. The temperature change in the primary treatment steps (grit chamber, pre-aeration and primary clarifiers) comprise 6% of the total. This is not insignificant and shows the importance of evaluating the temperature impacts plant-wide for accurate simulations of biological processes, for example in the ASU.

Figure 6(a) shows that the heat flux components with the greatest impact on average was  $\phi_{sr}$  and  $\phi_{bp}$  (positive) and  $\phi_{ar}$  and  $\phi_c$  (negative). The process with the clearest seasonal variation was  $\phi_{sr}$  (b), which follows the measured solar radiation (c). Also  $\phi_c$  and  $\phi_e$  showed variations from month to month with correlation to the outside temperature (a). The expression for  $\phi_c$  in the model reflects energy transfer for forced convection with mixed boundary layer conditions ( $2.5 \cdot 10^5 < Re < 1.5 \cdot 10^7$  with less than 10% of values  $< 5 \cdot 10^5$ ). While this provided the best fit to data of the alternatives tested (results not shown) for the presented case study, ambient conditions (e.g. wind speeds) in other cases might require altering this expression. For the energy contributions by biological reactions ( $\phi_{bp}$ ) the degradation of COD is dominating while nitrification and denitrification have smaller and similar impacts. During model development, the impact of rain

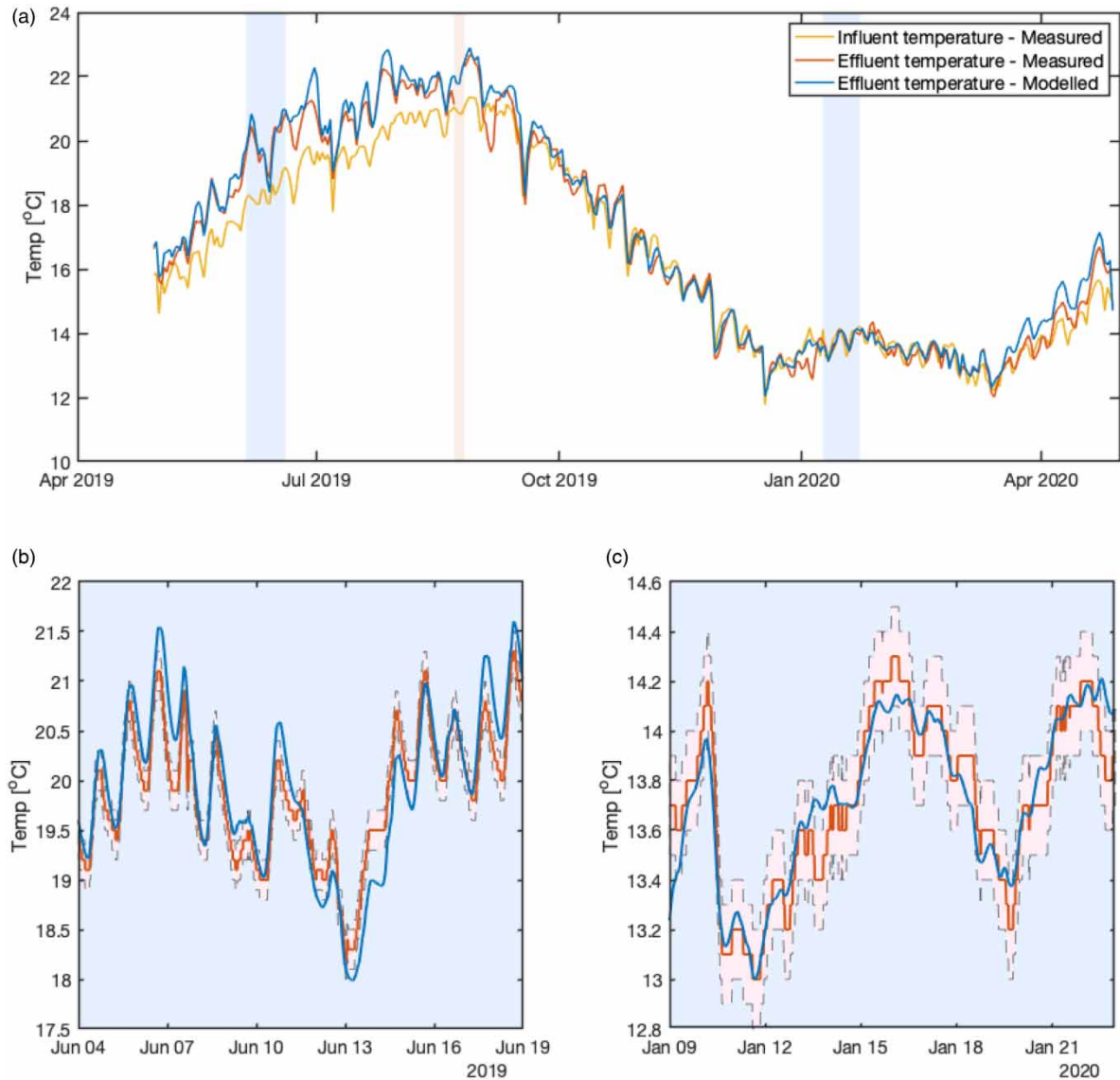


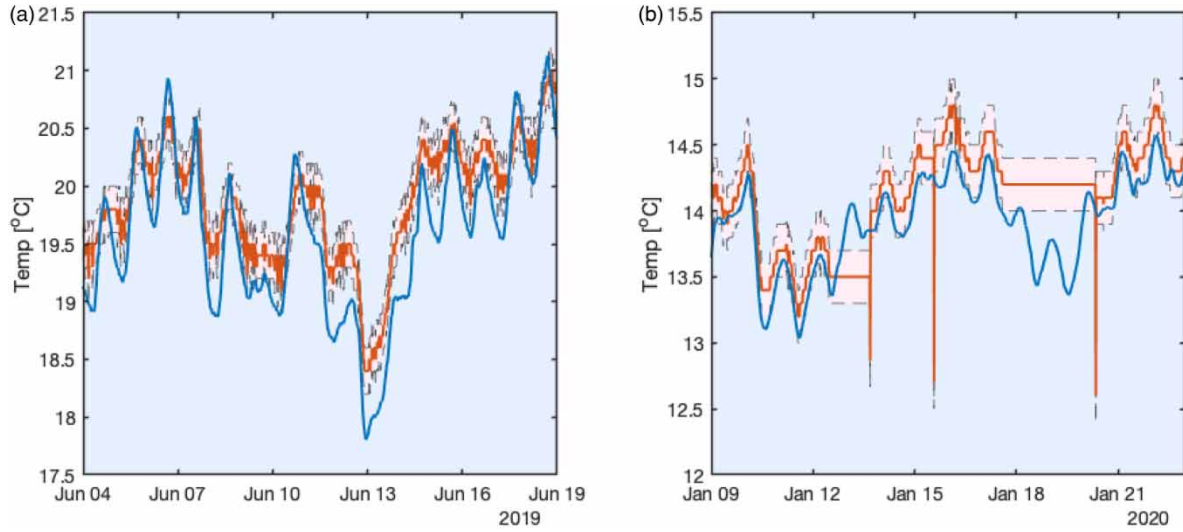
**Figure 3** | Measured influent and effluent temperature for the treatment plant along with simulated effluent temperature for the whole validation period (a) and selected periods for summer (b) and winter (c). In (a), the blue shaded area marks the selected periods and the red shaded area marks the period of partly corrupt data for the measured effluent temperature. In (b) and (c), the red shaded area between dashed grey lines mark the measurement uncertainty for the measured effluent temperature. Please refer to the online version of this paper to see this figure in colour: <http://dx.doi.org/10.2166/wst.2021.277>.

was evaluated. While storms heavily impact the influent flow and temperature (captured in influent data to the model) the rain over the uncovered tanks did not have a significant effect on temperature (data not shown).

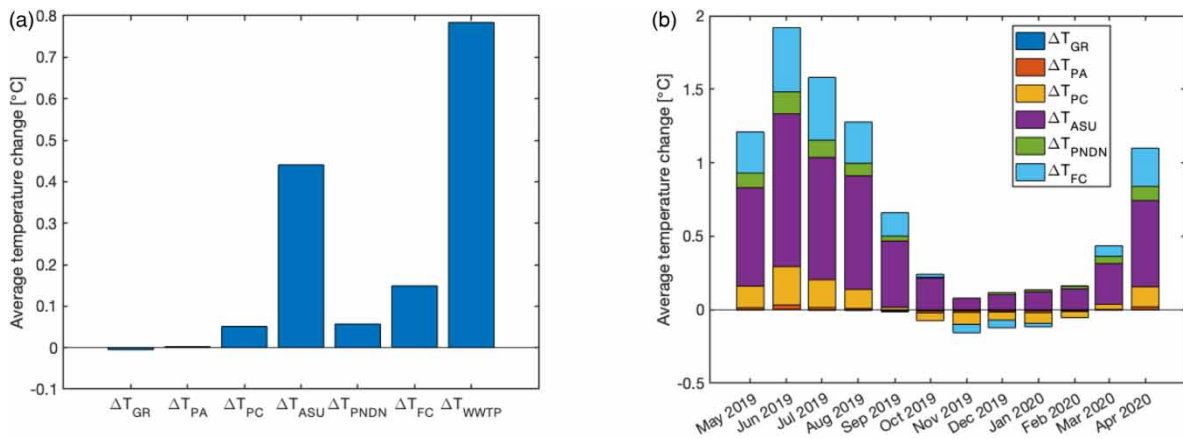
### Scenario analysis of wastewater heat recovery

Simulation results for Scenarios 1–3 are shown in Table 2 and Figure 7. The temperature increase over the plant was larger at lower influent temperatures, 1.0 °C in Scenario 3 compared to 0.8 °C for the default case. Considering the temperature in the ASU, which is critical for biological reaction rates, most of the temperature increase was attained there. When lowering the influent temperature 3 °C the temperature at the ASU effluent was reduced 2.8 °C.

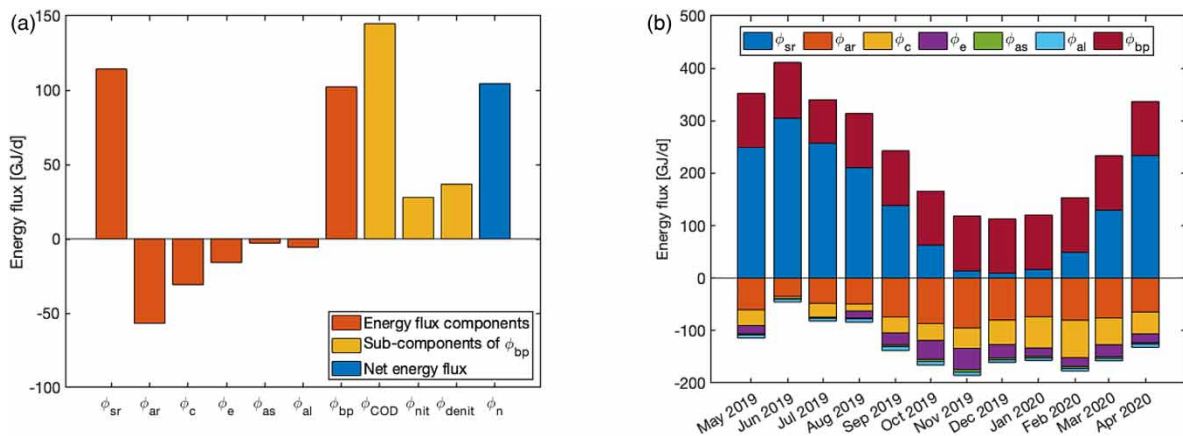
In the ASU, nitrification declines as temperatures drop. The annual average secondary effluent ammonia concentration increases from 4.9 mg/l in the default scenario to 7.5 mg/l in Scenario 3. However, the impact was not linear as temperatures dropped. The increase from the default case to Scenario 1 was 0.65 mg/l and from Scenario 2 to 3, it was 1.1 mg/l. The



**Figure 4** | Measured (red line) and modelled (blue line) temperature in the activated sludge reactors for selected periods during summer (a) and winter (b). The red shaded area between dashed grey lines mark the measurement uncertainty for the measured temperature. Please refer to the online version of this paper to see this figure in colour: <http://dx.doi.org/10.2166/wst.2021.277>.



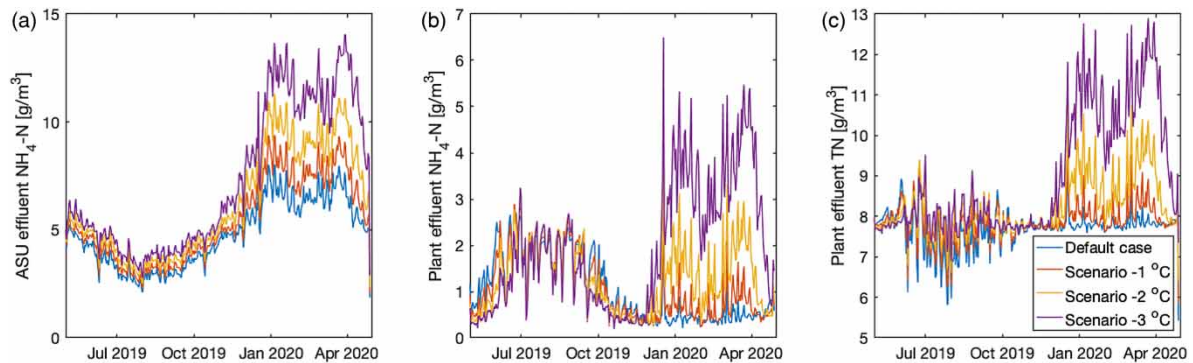
**Figure 5** | Average temperature change for the different sub-processes of the WWTP. Annual averages (a) and monthly averages (b).  $\Delta T$  indices: Grit removal (GR), Pre-aeration (PA), Primary clarifiers (PC), Activated sludge unit (ASU), Post nitrification and Post denitrification (PNDN), Final clarifiers (FC).



**Figure 6** | Energy fluxes for the different components of the heat flux equation (Equation (2)). Annual averages (a) and monthly averages (b).

**Table 2** | Annual average temperature (T) and nitrogen components in the activated sludge unit (ASU) effluent and plant effluent for the three scenarios reducing the influent temperature with 1, 2 and 3 °C compared to the default case

	Default	Scenario 1	Scenario 2	Scenario 3
T – Influent [°C]	16.5	15.5	14.5	13.5
NH <sub>4</sub> -N – ASU effluent [g N/m <sup>3</sup> ]	4.90	5.55	6.37	7.51
NO <sub>3</sub> -N – ASU effluent [g N/m <sup>3</sup> ]	7.91	7.98	7.93	7.66
TN – ASU effluent [g N/m <sup>3</sup> ]	14.0	14.7	15.6	16.5
T – ASU effluent [°C]	17.1	16.2	15.2	14.3
NH <sub>4</sub> -N – Plant effluent [g N/m <sup>3</sup> ]	0.973	1.02	1.27	1.94
NO <sub>3</sub> -N – Plant effluent [g N/m <sup>3</sup> ]	6.43	6.54	6.64	6.72
TN – Plant effluent [g N/m <sup>3</sup> ]	7.73	7.91	8.28	9.05
T – Plant effluent [°C]	17.3	16.4	15.5	14.5
ASU air flow [m <sup>3</sup> /d]	275,000	267,000	257,000	244,000
MBBR Ethanol dose [m <sup>3</sup> /d]	0.61	0.65	0.67	0.66

**Figure 7** | Dynamic simulation results (daily averages) for ammonia in the activated sludge unit (ASU) (a) and ammonia and total nitrogen in the plant effluent (b), (c) for the three scenarios reducing the influent temperature with 1, 2 and 3 °C compared to the default case.

seasonal variation was also strong (Figure 7(a)). While effluent ammonia concentrations were about the same for the three scenarios during summer, the increase was significant during winter.

The plant effluent shows a similar behaviour as the secondary effluent. The tertiary treatment with post nitrification and denitrification reduced some of the remaining ammonia and nitrate. In the plant effluent, the increase in ammonia was limited for Scenario 1, small for Scenario 2 but around 1 mg/l for Scenario 3. The post-nitrification step manages a slightly increased load of NH<sub>4</sub>-N but not fully for Scenario 3. The post-denitrification process (with nitrate control adjusting the ethanol dosage) was able to balance the nitrate levels in the effluent. The average total nitrogen in the effluent increased up to 9.1 mg/l (Scenario 3) compared to 7.7 mg/l for the default case while the ethanol addition increased by 8%. The annual average of 9.1 mg/l TN was below the plant effluent standard which is 10 mg/l for TN. However, the dynamic simulation (Figure 7(b) and 7(c)) revealed high peaks in both NH<sub>4</sub>-N and TN during winter. This would not be a desired process performance at any WWTP. For Scenario 1 and mostly for Scenario 2, the TN stayed below 10 mg/l also during winter.

The different temperatures and their impacts on the microbial nitrogen conversion processes in the ASU and MBBR led to changes in plant operation (Table 2). The plant controllers compensated for the changes in the processes. Primarily, the aeration in the ASU was reduced as less oxygen was consumed for nitrification and oxygen was more easily dissolved at the lower temperatures. Aeration was reduced by 3, 7 and 11% for Scenarios 1, 2 and 3, respectively, compared to the default case. Furthermore, the carbon addition control to the post-denitrification reactor compensated for the changes in nitrate load in the three scenarios. The carbon consumption increased for all scenarios with reduced temperature as more nitrogen was pushed to the tertiary treatment from the ASU. At the most, 11% more ethanol was dosed in Scenario 2 compared to the

default case. However, the trend was not distinct due to the sequential impacts on  $\text{NH}_4\text{-N}$  and  $\text{NO}_3\text{-N}$  concentrations from the ASU and post nitrification described above. As energy for aeration was a relatively larger cost than external carbon source (5,940 compared to 4,350 cost units per day for the default case using the operational cost index equations from BSM2), the savings on aeration exceeded the increased expenditure for denitrification.

### Model application and limitations

The integrated temperature and process model presented did show good accuracy for the intended use of evaluating WWHR options. Compared to previously presented models (Sedory & Stenstrom 1995; Makinia *et al.* 2005; Lippi *et al.* 2009), the set of heat flux equations and corresponding parameters were proven valid for full-year simulations of WWTPs also in colder climate conditions (i.e. temperate climate). The primary and tertiary treatment steps had a significant impact on the temperature, meaning that plant-wide modelling is essential when evaluating the impact of small temperature changes as seen with WWHR. The model does not include an actual heat balance for the AD as its temperature is controlled by heating all year. In situations where this is not the case a heat balance for the AD needs to be added. The model is easily integrated with general WW process models (no interfaces or modifications of the existing models are required) and the required meteorological data can be measured locally using standard weather stations. This allows the model to be used for a wide range of cases where accurate temperature predictions are of importance. Also, implementing the equations in existing WWTP models is possible where the modelling software allows coding of user defined equations, e.g. expanding the model in commercial simulation platforms regardless of platform and model framework for existing process models. The model is intended and validated for uncovered outdoor tanks and not for covered or indoor/underground treatment plants. The model has been validated for ambient temperatures from  $-2.5$  to  $25$  °C. For arctic climate with strong sub-zero temperatures, it is recommended to revalidate the model parameters.

## CONCLUSIONS

Heat balances have been implemented in a plant-wide wastewater treatment plant process model and, in contrast to previous work, validated for a wastewater treatment plant in a temperate climate for a full year of dynamic simulation. A novel set of dynamic expressions was applied for the consecutive equations and parameters of the heat balance model to allow for temperature predictions throughout the plant and over the wide temperature range at the location. The key findings from the modelling and simulation study are as follows:

1. The model predicts effluent and in-tank water temperature with a good fit to measured data. The temperature change from influent to effluent is on an average  $0.78$  °C of which  $0.35$  (45%) arise from other processes than the ASU. This shows the importance of evaluating the temperature impacts plant-wide for accurate simulations of wastewater heat recovery and biological process performance.
2. From dynamic simulations and validation, it is evident that the temperature impact is not constant over the year. Dynamic parameters are necessary in the heat flux equations to be able to predict temperature impact in periods of both warm and cold conditions.
3. The energy processes which have the largest energy contribution are solar radiation and biological processes, while the largest losses are due to atmospheric radiation along with conduction and convection.
4. Tanks with large open surface areas have significant impact on the heat balance regardless of biological processes.
5. When varying the influent temperature up to  $3$  °C, the impact on the in-tank temperature of the ASU is  $2.8$  °C, which has a significantly negative impact on nitrogen removal. Total nitrogen annual average in the secondary effluent increases from  $14$  to  $16.5$  mg/l and in the plant effluent from  $7.7$  to  $9.1$  mg/l. At the same time aeration requirement is reduced by up to 11% in the activated sludge and carbon source dosing for post denitrification increases by up to 11%. Overall, the operational cost decreases with temperature. This shows the necessity for plant specific and plant-wide evaluations.

## ACKNOWLEDGEMENTS

The authors acknowledge the financial support provided by the Swedish research council Formas (942-2016-80), The Swedish Water and Wastewater Association (16-106), Sweden Water Research, Kåppalaförbundet and Tekniska Verken in Linköping for the project HÅVA ('Sustainability analysis for heat recovery from wastewater'). Tekniska Verken in Linköping, is also gratefully acknowledged for their financial support and for supporting measurement campaigns.

## DATA AVAILABILITY STATEMENT

All relevant data are available from an online repository or repositories.

## REFERENCES

- Arnell, M., Lundin, E. & Jeppsson, U. 2017 *Sustainability Analysis for Wastewater Heat Recovery – Literature Review*. Report TEIE-7267, Division of Industrial Electrical Engineering and Automation, Lund University, Lund, Sweden.
- Baeten, J. E., Batstone, D. J., Schraa, O. J., van Loosdrecht, M. C. M. & Volcke, E. I. P. 2019 *Modelling anaerobic, aerobic and partial nitrification-anammox granular sludge reactors – a review*. *Water Research* **149**, 322–341.
- Belia, E., Amerlinck, Y., Benedetti, L., Johnson, B., Sin, G., Vanrolleghem, P. A., Gernaey, K. V., Gillot, S., Neumann, M. B., Rieger, L., Shaw, A. & Villez, K. 2009 *Wastewater treatment modelling: dealing with uncertainties*. *Water Science and Technology* **60** (8), 1929–1941.
- Blackburn, J. W. & Cheng, J. 2005 *Heat production profiles from batch aerobic thermophilic processing of high strength swine waste*. *Environmental Progress* **24** (3), 323–333.
- Bolz, R. E. & Tuve, G. L. 1976 *CRC Handbook of Tables for Applied Engineering Science*. CRC Press, Boca Raton, FL, USA.
- Bower, S. M. & Saylor, J. R. 2009 *A study of the Sherwood-Rayleigh relation for water undergoing natural convection-driven evaporation*. *International Journal of Heat and Mass Transfer* **52** (13–14), 3055–3063.
- Ceconet, D., Racek, J., Callegari, A. & Hlavinec, P. 2020 *Energy recovery from wastewater: a study on heating and cooling of a multipurpose building with sewage-reclaimed heat energy*. *Sustainability* **12** (116), 1–11.
- Culha, O., Gunerhan, H., Biyik, E., Ekren, O. & Hepbasli, A. 2015 *Heat exchanger applications in wastewater source heat pumps for buildings: a key review*. *Energy and Buildings* **104**, 215–232.
- Fernandez-Arevalo, T., Lizarralde, I., Grau, P. & Ayesa, E. 2014 *New systematic methodology for incorporating dynamic heat transfer modelling in multi-phase biochemical reactors*. *Water Research* **60**, 141–155.
- Fernandez-Arevalo, T., Lizarralde, I., Fdz-Polanco, F., Perez-Elvira, S. I., Garrido, J. M., Puig, S., Poch, M., Grau, P. & Ayesa, E. 2017 *Quantitative assessment of energy and resource recovery in wastewater treatment plants based on plant-wide simulations*. *Water Research* **118**, 272–288.
- Gernaey, K. V., Jeppsson, U., Vanrolleghem, P. A. & Copp, J. B. 2014 *Benchmarking of Control Strategies for Wastewater Treatment Plants*. IWA Scientific and Technical Report No. 21. IWA Publishing, London, UK.
- Griffiths, C. 2012 *A Thermodynamic Analysis of Biological Systems Using Process Synthesis*. Thesis PhD, Faculty of Engineering and the Built Environment, University of the Witwatersrand, Johannesburg, South Africa.
- Henze, M., Gujer, W., Mino, T. & van Loosdrecht, M. C. M. 2000 *Activated Sludge Models ASM1, ASM2, ASM2d and ASM3*. IWA Scientific and Technical Report No. 9. IWA Publishing, London, UK.
- Henze, M., Harremoës, P., la Cour Jansen, J. & Arvin, E. 2002 *Wastewater Treatment: Biological and Chemical Processes*. Springer Science and Business Media, Berlin, Germany.
- Henze, M., van Loosdrecht, M. C. M., Ekama, G. A. & Brdjanovic, D. 2008 *Biological Wastewater Treatment – Principles, Modelling and Design*. IWA Publishing, London, UK.
- Hiatt, W. C. & Grady, C. P. L. 2008 *An updated process model for carbon oxidation, nitrification, and denitrification*. *Water Environment Research* **80** (11), 2145–2156.
- Huber, M. L., Perkins, R. A., Laesecke, A., Friend, D. G., Sengers, J. V., Assael, M. J., Metaxa, I. N., Vogel, E., Mares, R. & Miyagawa, K. 2009 *New international formulation for the viscosity of H<sub>2</sub>O*. *Journal of Physical and Chemical Reference Data* **38** (2), 101–125.
- Incropera, F. P., Lavine, A. S., Bergman, T. L. & DeWitt, D. P. 2007 *Fundamentals of Heat and Mass Transfer*. John Wiley & Sons Inc, Hoboken, NJ, USA.
- Jonsson, R., Sundén, T., Bengtsson, L. & Kristoffersson, J. 2020 *Värmeåtervinningssystem för spillvatten i flerbostadshus [Systems for Heat Recovery From Wastewater in Multi-Family Houses (in Swedish)]*. Sustainable Innovation AB, Stockholm, Sweden.
- Kleerebezem, R. & van Loosdrecht, M. C. M. 2010 *A generalized method for thermodynamic state analysis of environmental systems*. *Critical Reviews in Environmental Science and Technology* **40** (1), 1–54.
- la Cour Jansen, J., Kristensen, G. H. & Laursen, K. D. 1992 *Activated sludge nitrification in temperate climate*. *Water Science and Technology* **25** (4–5), 177–184.
- Lippi, S., Rosso, D., Lubello, C., Canziani, R. & Stenstrom, M. K. 2009 *Temperature modelling and prediction for activated sludge systems*. *Water Science and Technology* **59** (1), 125–131.
- Makinia, J., Wells, S. A. & Zima, P. 2005 *Temperature modeling in activated sludge systems: a case study*. *Water Environment Research* **77** (5), 525–532.
- Melcer, H., Dold, P. L., Jones, R. M., Bye, C. M., Takács, I., Stensel, H. D., Wilson, A. W., Sun, P. & Bury, S. 2003 *Methods for Wastewater Characterization in Activated Sludge Modelling*. Water Environment Federation and IWA Publishing, Alexandria, VA, USA and London, UK.
- Nellis, G. & Klein, S. 2012 *Heat Transfer*. Cambridge University Press. NY, USA, New York.
- Olsson, G. 2012 *Water and Energy – Threats and Opportunities*. IWA Publishing, London, UK.
- Otterpohl, R. & Freund, M. 1992 *Dynamic models for clarifiers of activated sludge plants with dry and wet weather flows*. *Water Science and Technology* **26** (5–6), 1391–1400.

- Rasmussen, K. 1997 *Calculation Methods for the Physical Properties of air Used in the Calibration of Microphones. Report PL-11b, 1997.* Technical University of Denmark, Copenhagen, Denmark.
- Rieger, L., Gillot, S., Langergraber, G., Ohtsuki, T., Shaw, A., Takács, I. & Winkler, S. 2012 *Guidelines for Using Activated Sludge Models. IWA Scientific and Technical Report No. 22.* IWA Publishing, London, UK.
- Sedory, P. E. & Stenstrom, M. K. 1995 *Dynamic prediction of waste-water aeration basin temperature. Journal of Environmental Engineering* **121** (9), 609–618.
- Swedish Energy Agency 2009 *Mätning av kall- och varmvattenanvändning i 44 hushåll [Measurements of Cold and Hot Water Use in 44 Households (in Swedish)]. Report ER 2009:26.* Swedish Energy Agency, Eskilstuna, Sweden.
- Tsilingiris, P. T. 2018 *Review and critical comparative evaluation of moist air thermophysical properties at the temperature range between 0 and 100 °C for engineering calculations. Renewable & Sustainable Energy Reviews* **83**, 50–63.
- Verstraete, W., de Caveye, P. V. & Diamantis, V. 2009 *Maximum use of resources present in domestic ‘used water’. Bioresource Technology* **100** (23), 5537–5545.
- Wärff, C., Arnell, M., Jeppsson, U. & Sehlén, R. 2020 *Modelling heat recovery potential from household wastewater. Water Science and Technology* **81** (8), 1597–1605.
- Zaborowska, E., Czerwionka, K. & Makinia, J. 2021 *Integrated plant-wide modelling for evaluation of the energy balance and greenhouse gas footprint in large wastewater treatment plants. Applied Energy* **282**, 116126.

First received 7 May 2021; accepted in revised form 1 July 2021. Available online 14 July 2021